NANO LETTERS

March 2019
Volume 19, Number 3
pubs.acs.org/NanoLett

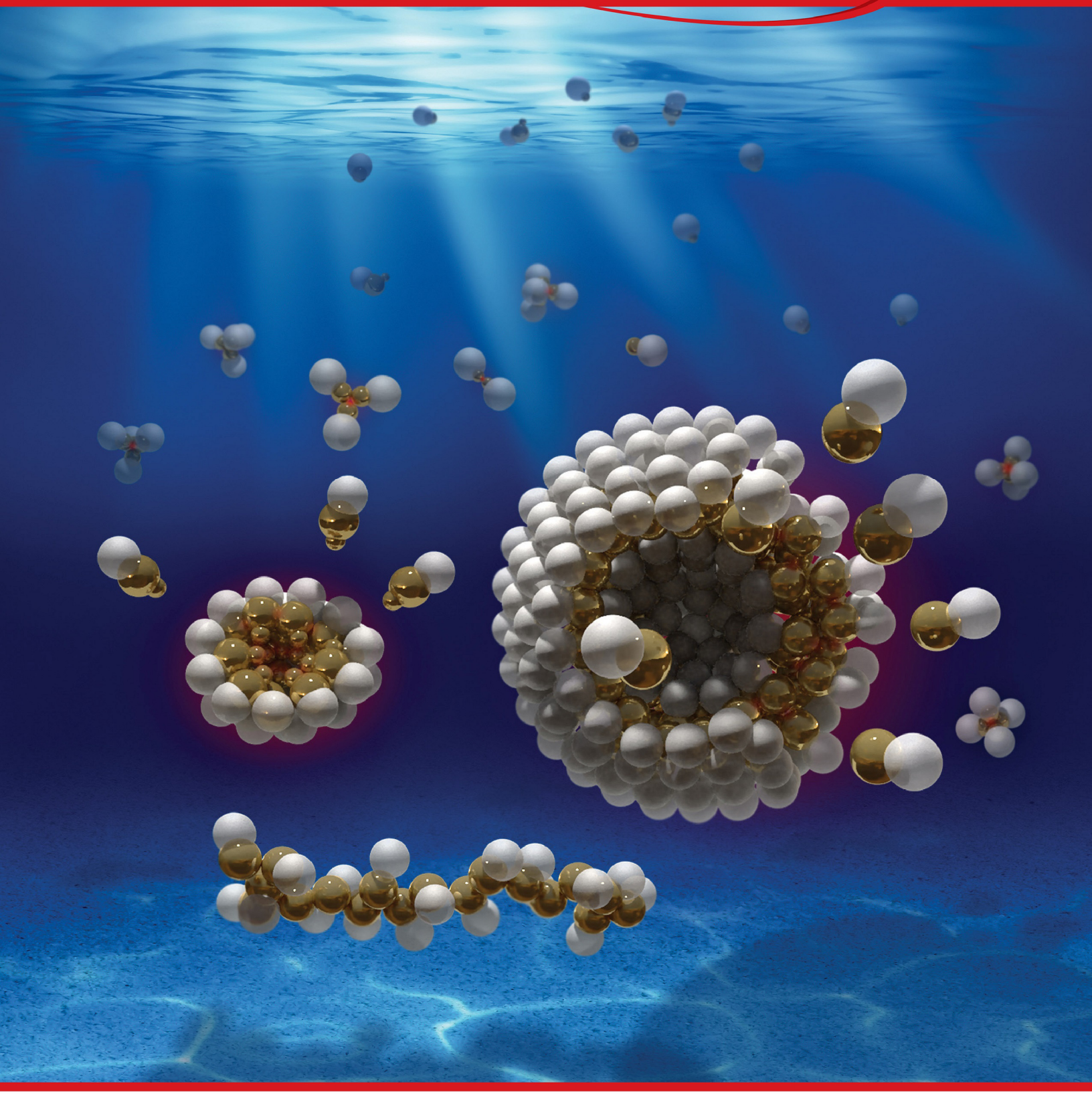

NANO LETTERS
Cite This: Nano Lett. XXXX, XXX, XXX−XXX
Letter
pubs.acs.org/NanoLett

Self-assembly of Janus Dumbbell Nanocrystals and Their Enhanced Surface Plasmon Resonance

Fei Liu,[†] Shailja Goyal,[‡] Michael Forrester,[‡] Tao Ma,[§] Kyle Miller,[†] Yasmeen Mansoorieh,[†] John Henjum,[†] Lin Zhou,[†,§] Eric Cochran,[‡] and Shan Jiang*[,†,§]

[†]Department of Materials Science and Engineering and [‡]Department of Chemical and Biological Engineering, Iowa State University, Ames, Iowa 50011, United States

[§]Division of Materials Science and Engineering, Ames National Laboratory, Ames, Iowa 50011, United States

Supporting Information

ABSTRACT: Self-assembly is a critical process that can greatly expand the existing structures and lead to new functionality of nanoparticle systems. Multicomponent superstructures self-assembled from nanocrystals have shown promise as multifunctional materials for various applications. Despite recent progress in assembly of homogeneous nanocrystals, synthesis and self-assembly of Janus nanocrystals with contrasting surface chemistry remains a significant challenge. Herein, we designed a novel Janus nanocrystal platform to control the self-assembly of nanoparticles in aqueous solutions by balancing the hydrophobic and hydrophilic moieties. A series of superstructures have been assembled by systematically varying the Janus balance and assembly conditions. Janus Au−Fe_3O_4 dumbbell nanocrystals (<20 nm) were synthesized with the hydrophobic ligands coated on the Au lobe and negatively charged hydrophilic ligands coated on the Fe_3O_4 lobe. We systematically fine-tune the lobe size ratio, surface coating, external conditions, and even additional growth of Au nanocrystal domains on the Au lobe of dumbbell nanoparticles (Au−Au−Fe_3O_4) to harvest self-assembly structures including clusters, chains, vesicles, and capsules. It was discovered that in all these assemblies the hydrophobic Au lobes preferred to stay together. In addition, these superstructures clearly demonstrated different levels of enhanced surface plasmon resonance that is directly correlated with the Au coupling in the assembly structure. The strong interparticle plasmonic coupling displayed a red-shift in surface plasmon resonance, with larger structures formed by Au−Au−Fe_3O_4 assembly extending into the near-infrared region. Self-assembly of Janus dumbbell nanocrystals can also be reversible under different pH values. The biphasic Janus dumbbell nanocrystals offer a platform for studying the novel interparticle coupling and open up opportunities in applications including sensing, disease diagnoses, and therapy.

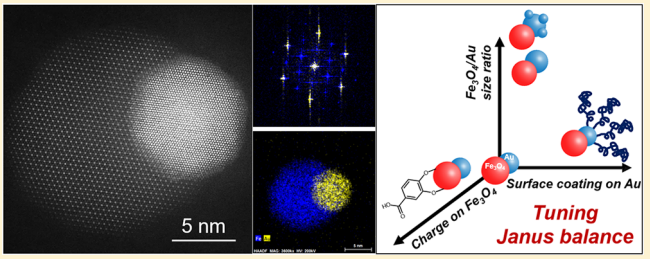

KEYWORDS: *Janus nanoparticles, self-assembly, Janus balance, superstructures, plasmonic coupling*

The principles of self-assembly govern many aspects of life in nature as the process provides versatile properties using simple building blocks.[1] The same principles can also be applied to fabricate hierarchical structures with diverse functionalities.[2−4] For example, small surfactant and lipid molecules assemble into a variety of structures including micelles and vesicles with a simple amphiphilic motif. These structures have important functionality in biology and applications in industry. Another example is polymers with a diblock architecture that assemble into unique phases.[5] By adjusting the block size and interactions among segments, the assembly structures go through spherical, cylindrical, gyroid, and lamellar phases. However, conventional nanoparticles and colloids have homogeneous surfaces and therefore only interact isotropically during the assembly process. Breaking the symmetry of particles will introduce directional interactions and lead to novel structures. One great example is Janus particle, named after the Roman god, which has different chemistries on the two sides of a single particle.[6] Janus particles in micron size were observed to assemble into many fascinating structures including well-defined clusters, helical fibril-like chains and two-dimensional crystals with hydrophobic stripes.[7−9] Theory and simulation further illustrated that the Janus balance (surface ratio between the two sides of the Janus particles) played a key role in determining the assembly behaviors.[10,11] More interestingly, external stimuli, such as ionic strength,[12,13] light,[14,15] pH,[16] and magnetic/electric field,[17−20] can change the assembly structures of Janus particles, demonstrating their great potential in fabricating smart materials that are responsive to the environment.

It is speculated that the same assembly principles would hold for Janus nanoparticles of much smaller size, which bridge the length scale of small surfactant molecules and microsized

Received: November 5, 2018
Revised: December 20, 2018
Published: December 26, 2018

DOI: 10.1021/acs.nanolett.8b04464
Nano Lett. XXXX, XXX, XXX−XXX

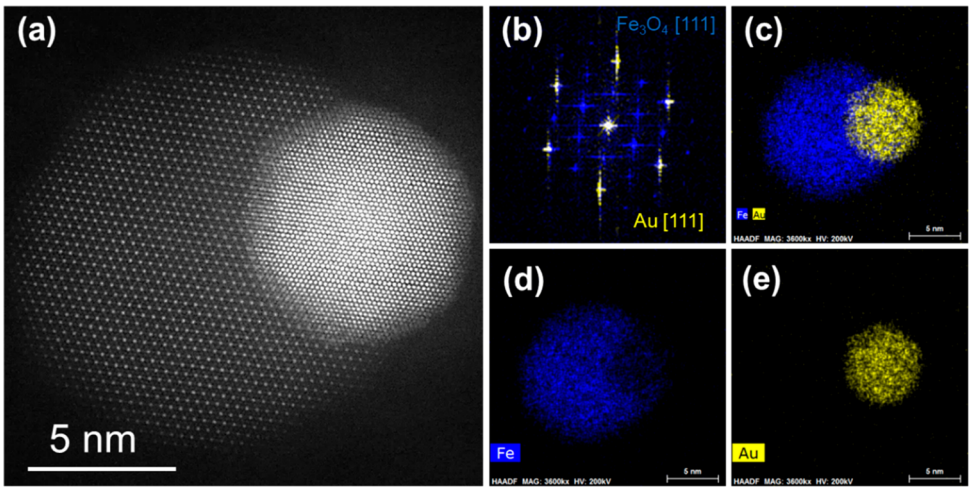

Figure 1. (a) HAADF-STEM image of a typical Au−Fe_3O_4 nanocrystal. (b) The overlaid fast FFT patterns of Au and Fe_3O_4 lobes. (c−e) EDS elemental mapping of a single Au−Fe_3O_4 nanocrystal.

particles. The synthesis of Janus nanoparticles has been extensively developed in the past decades.[7,21−25] However, no systematic studies have been carried out on amphiphilic Janus nanoparticle assembly with different Janus balance in simple aqueous suspensions. Previous research has focused on the template-mediated or solution-based surface modification of single-component nanoparticles, such as Au and Fe_3O_4 nanoparticles.[26−28] Many of these systems require intensive efforts on ligand preparation, stepwise surface modification, and surface segregation control. In addition, it is extremely difficult to directly observe the ligand distribution and Janus nanoparticle orientation with this system. On the other hand, dumbbell nanoparticles offer a straightforward route to fabricate Janus nanoparticles with two lobes reacting differently with the potential ligands.[29−32] However, it still remains challenging to stabilize these nanoparticles in aqueous suspensions and systematically vary the morphology and surface functionality of the dumbbell nanoparticles over a wide range. In particular, it is very difficult to achieve a more dominant hydrophobic lobe, since enlarging the hydrophobic lobe will destabilize nanoparticles during the synthesis and agglomerate Janus dumbbell nanoparticles into random aggregates in solution.

In order to address these challenges, we developed a simple platform based on Janus dumbbell nanocrystals composed of Au and Fe_3O_4 lobes. Homogeneous Au and Fe_3O_4 nanocrystals have been widely studied because both materials are biocompatible and possess unique properties. Dumbbell nanocrystals fabricated using these two materials are promising candidates for various applications. In addition, the two different lobes with distinct surface reactivity provide a reliable approach to asymmetrically functionalize the dumbbell nanoparticles. We then demonstrated the capability to control the self-assembly of Janus nanoparticles by fine-tuning the Janus balance through lobe size, surface coating, and surface charges. This systematic change in Janus balance results in a variety of superstructures. Furthermore, both polymer grafting and Au lobe extension by growing additional Au nanodomains were developed to further enlarge the hydrophobic side. The bigger hydrophobic lobes direct the assembly to larger and more sophisticated structures (vesicle and capsules), which in turn leads to enhanced surface plasmon resonance with adsorption extending into the near-infrared range. The results are in general agreement with the previous studies for amphiphilic Janus spheres in micron size, although the specific arrangement of particles are not exactly the same.[33] With the coating of carboxylic acid groups on the Fe_3O_4 lobe, we further demonstrate that the Janus dumbbell nanocrystals can be reversibly assembled under different pH conditions. Our new Janus nanoparticle platform provides a guideline for the design of more complex superstructures and opens up new opportunities in applications including sensing, separation, drug delivery, and disease diagnoses.

Au−Fe_3O_4 dumbbell nanocrystals coated by oleylamine and oleic acid were synthesized by growing a second lobe of Fe_3O_4 on the preformed Au nanocrystals in solution. Because of the long carbon chain attached on the lobe surface, Au−Fe_3O_4 nanoparticles could be well dispersed in various nonpolar solvents such as hexane, toluene, and chloroform. Figure 1a shows the high-angle annular dark-field scanning transmission electron microscopy (HAADF-STEM) image of a typical Au−Fe_3O_4 nanoparticle, which clearly indicates its dumbbell-like morphology and high crystallinity in both lobes. Au is partially covered by Fe_3O_4 and is much brighter compared to Fe_3O_4 in the image due to its higher atomic number (Z-contrast in HAADF). Both lobes are oriented along the ⟨111⟩ zone axis, providing a clear hexagonal projection. The overlaid fast Fourier transform (FFT) patterns of each lobe (Figure 1b) confirms $\langle 111\rangle_{Au}$ //$\langle 111\rangle_{Fe3O4}$ epitaxial relationship. The unit cell of Fe_3O_4 is matched by 2 × 2 gold unit cells with the lattice mismatch of 2.8%, allowing epitaxial growth of Fe_3O_4 on Au. Corresponding energy-dispersive X-ray spectroscopy (EDS) elemental mapping (Figure 1c−e) further reveals the chemical distribution within the Janus Au−Fe_3O_4 nanocrystal.

The well-defined Au−Fe_3O_4 dumbbell morphology enables us to differentiate two different lobes and modify the lobe surfaces with hydrophilic and hydrophobic ligands to render the nanocrystal amphiphilic. Through a ligand exchange process, 3,4-dihydroxybenzoic acid was strongly anchored onto Fe_3O_4 via a five-membered metallocyclic chelate. The modified Fe_3O_4 lobe is terminated with carboxylic group, providing the necessary charge to stabilize the particles in aqueous solution. On the other hand, the Au lobe was protected by pristine oleylamine or thiols (e.g., 1-octadecanethiol) through Au−S chemistry, keeping its hydrophobicity. As a result, the negatively charged Fe_3O_4 lobes will repel each

DOI: 10.1021/acs.nanolett.8b04464
Nano Lett. XXXX, XXX, XXX−XXX

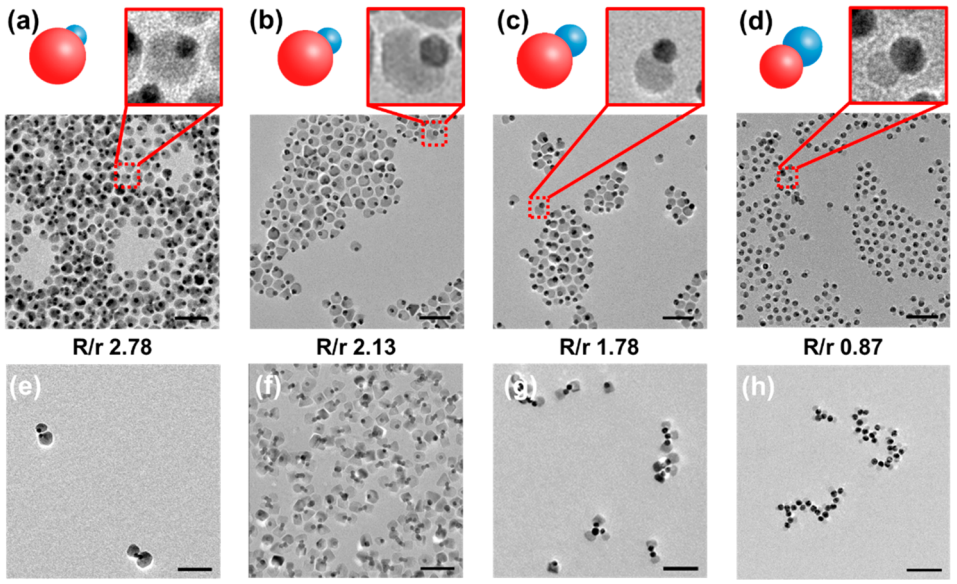

Figure 2. Au−Fe_3O_4 dumbbell nanocrystals with different lobe size ratios in (a−d) organic solvent and (e−h) aqueous solutions correspondingly (all scale bars are 50 nm).

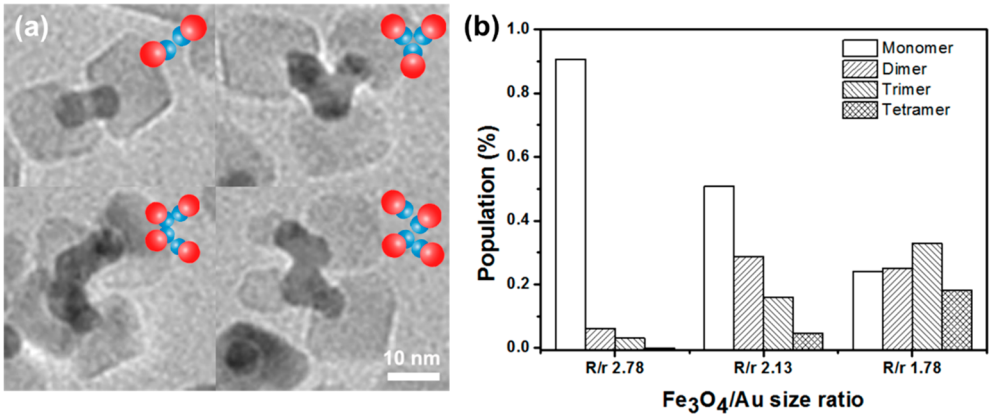

Figure 3. (a) Clusters consisting of 2, 3, and 4 dumbbell nanocrystals. (b) Cluster size distribution with different Fe_3O_4/Au size ratios.

other by electrostatic interactions, while hydrophobic Au lobes attract each other due to hydrophobic and strong van der Waals interactions. Therefore, the balance between hydrophobic Au and hydrophilic Fe_3O_4 becomes essential for tuning the interactions that lead to self-assembly of Janus Au−Fe_3O_4 nanocrystals. We carefully controlled the Janus balance using four strategies: changing hard lobe size ratio (Fe_3O_4/Au size ratio), grafting molecules of different dimensions on the on the hydrophobic Au lobes, turning surface charges on Fe_3O_4 by adjusting the pH in solutions, and growing additional Au nanodomains on the Au lobe.

The first strategy to control self-assembly of Janus Au−Fe_3O_4 dumbbell nanocrystals is changing the Fe_3O_4/Au lobe size ratio. Because the ligands on both Au and Fe_3O_4 lobes are orders of magnitude smaller than the lobe diameters, the Janus balance of Au−Fe_3O_4 nanoparticles is mostly determined by the size of the hard core of the dumbbell nanoparticles. By varying the size of Au seed and reaction duration in the lobe growth, the Fe_3O_4/Au lobe size ratio was effectively tuned from 2.78 to 0.87 (Figure 2). Larger Au seed nanoparticles and shorter reaction duration for Fe_3O_4 growth at high temperature could facilitate the formation of Au−Fe_3O_4 dumbbell nanocrystals with smaller Fe_3O_4/Au lobe size ratios. TEM images in Figure 2a−d also confirm that all Au−Fe_3O_4 dumbbell nanocrystals before surface ligand exchange are randomly oriented when dried from the nonpolar solvent due to the lack of directional interactions. However, after surface ligand exchange and transfer to the aqueous solutions, the Au lobes of the Janus dumbbell nanocrystals prefer to stay together when dried. Obviously, this is due to the hydrophobic and van der Waals interactions between the Au lobes.

More interestingly, Janus Au−Fe_3O_4 nanocrystals with different lobe size ratios exhibit distinct self-assembly behavior, leading to clusters of different sizes (Figure 2e−h). It is challenging to test the ultimate stability of the assembly structures, however, from TEM observation and UV−vis measurement all the clusters remained stable for at least one month. When the Au lobe is small (Fe_3O_4/Au lobe size ratio of 2.78), a small fraction of particles form dimers with their Au lobes facing each other. Decreasing the Fe_3O_4/Au lobe size ratio from 2.78 to 1.78 results in the gradual emergence of trimers and tetramers. More detailed features of the clusters are provided in Figure 3a. Cluster size distribution shown in Figure 3b indicates that the population distribution of assembled dimers, trimers, and tetramers are controlled by the lobe size ratio. Most of the Janus Au−Fe_3O_4 nanocrystals remain as

DOI: 10.1021/acs.nanolett.8b04464
Nano Lett. XXXX, XXX, XXX−XXX

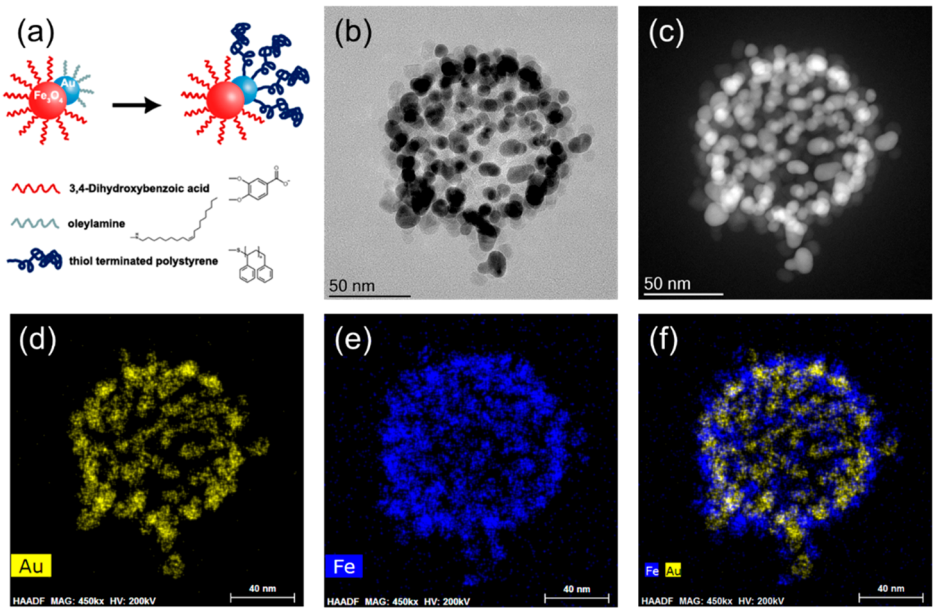

Figure 4. (a) Scheme of ligand exchange for polystyrene polymers onto the Au lobe; (b-c) TEM analyses of assembly structures of Janus dumbbell nanocrystals coated with polystyrene: (b) bright-field TEM image, (c) HAADF-STEM image, and EDS elemental mapping for (d) Au, (e) Fe and (f) Fe+Au.

individual nanoparticles when the lobe size ratio is 2.78, where trimers and tetramers are very rare. A small decrease in the lobe size ratio to 2.13 facilitates the assembly by attractions between Au lobes, drastically decreasing the fraction of individual Janus nanoparticles. The amount of larger clusters (e.g., tetramers) is also increased. More importantly, when the lobe size ratio decreases further to 1.16 and 0.87, pentamers and even long chains were observed in the assembled structures (Figure 2h and Figure S1). It is very obvious that increasing the hydrophobic Au lobe size can lead to larger cluster and long chain structures comprising more dumbbell nanocrystals. A larger hydrophobic lobe offers stronger Au−Au attractions and more surfaces for the Au lobe to contact with each other, which leads to subsequent bigger structures. The same trend was discovered in the previous studies on Janus spheres of micron size albeit at completely different length scales.[33] This implies that models used to describe Janus spheres at micron size might be adopted to study these dumbbell nanocrystals (~20 nm). However, the length scales of the interactions need be taken into account to explain the variations in assembly structures, as well as the other notable differences between dumbbell nanocrystals and micron-sized Janus spheres. The dumbbell nanocrystals have an elongated morphology rather than the spherical shape. When forming chains, Janus spheres form helical fibril-like structures, whereas dumbbell nanocrystals form simple extended chains with the Au lobe connecting with each other. The assembly structures for dumbbell nanocrystals were only observed under dried condition, and structures in aqueous suspensions could be different.

The second strategy to change Janus balance is by grafting molecules of different sizes on the dumbbell nanoparticles. Although the Au−Fe_3O_4 lobe size ratio effectively controls self-assembly of Janus Au−Fe_3O_4 dumbbell nanocrystals and produces a series of interesting superstructures, it is extremely challenging to push the Fe_3O_4/Au lobe size ratio much lower by direct solution synthesis. In fact, a lobe size ratio as low as the 0.87 in our work is scarcely reported. In order to further lower the ratio, Au seed nanocrystals as large as 14 nm were synthesized, and the reaction duration for Fe_3O_4 growth at high temperature was controlled for less than 15 min. However, the synthesis resulted in bad morphology and random aggregation, which was probably due to the poor stability of large Au nanocrystals at high temperature. An alternative to further increase the hydrophobic moiety of the Janus dumbbell nanoparticle is capping the Au lobe with a larger hydrophobic ligand. As illustrated in Figure 4a, thiol-terminated polystyrene with precise molecular weight (M_n) synthesized by living radical polymerization was used to replace the small oleylamine on the Au lobe. The catechol modification and self-assembly processes were kept the same. Previous studies have demonstrated that polymer brushes with different molecular weight (M_n) on nanocrystals could induce different assemblies.[34−36] The thickness of polystyrene brush on Au nanoparticles in good solvents (e.g., toluene and dimethylformamide) was found directly proportional to the M_n.[36] The trend is expected to be consistent in aqueous solutions although the power law could be different, because polystyrene will shrink and segregate on the nanoparticle surface in poor solvent. Polystyrene with a higher M_n is expected to form a thicker brush on Au lobe and induce stronger attraction between Au lobes due to the increased hydrophobicity.[37,38] More importantly, the thicker polystyrene layer will further enlarge the effective size of the hydrophobic lobe and change the Janus balance of the dumbbell nanocrystals. Although the thicker polystyrene layer may space out the nanoparticles and reduce the short-ranged van der Waals interaction between the Au lobes, the increase in long-range hydrophobic attraction seems more dominant during the assembly process. We observed that similar clusters and chains were formed when M_n is small, indicating the attraction between polystyrene-grafted Au lobes was similar to those covered by small hydrophobic molecules. Notably, when M_n reaches 10 000 g/mol vesicle-like assembly structures emerge, as shown in Figure 4. TEM (Figure 4b) and HAADF-STEM (Figure 4c) images indicate a collapsed hollow spherical

DOI: 10.1021/acs.nanolett.8b04464
Nano Lett. XXXX, XXX, XXX−XXX

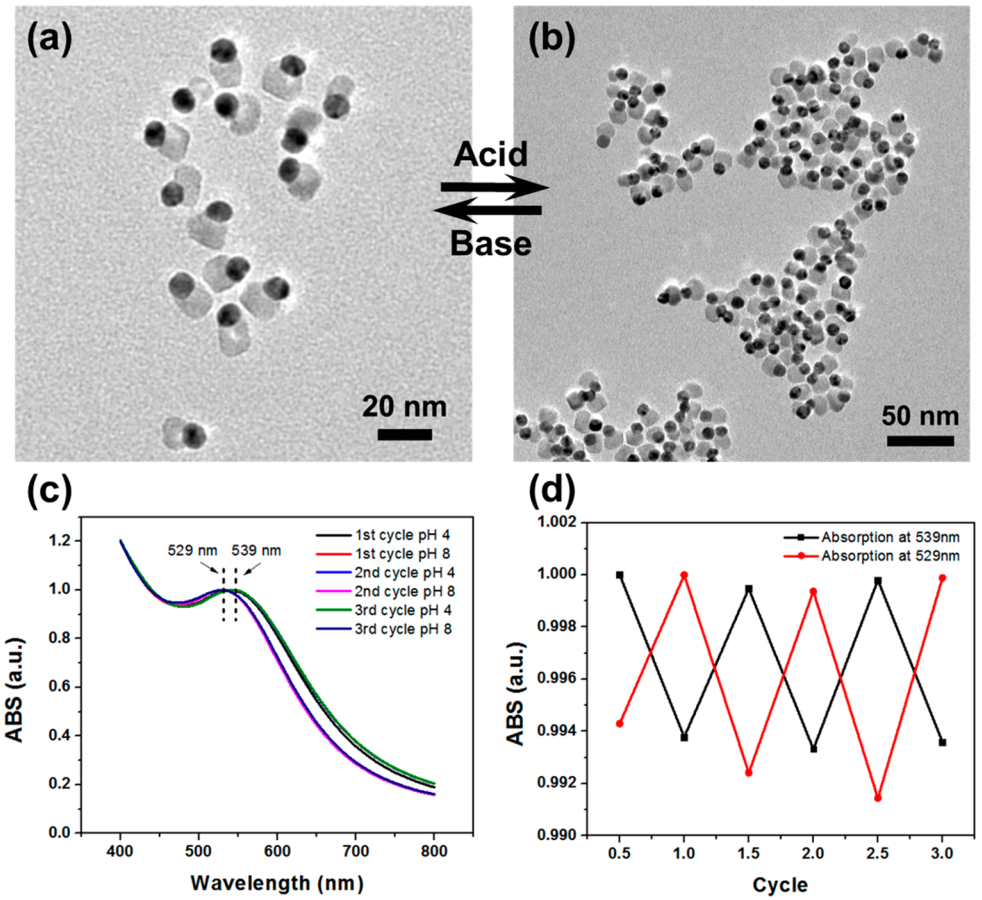

Figure 5. (a) Janus dumbbell nanocrystals dried from solution of pH = 8. (b) Janus dumbbell nanocrystals dried from solution of pH = 4. (c) UV−vis spectra of Janus dumbbell nanocrystals cycled between pH = 4 and 8. (d) The adsorption intensity at 538 and 529 nm when Janus dumbbell nanocrystals cycled between pH = 4 and 8.

structure in which Au lobes tend to stay with each other. EDS elemental mapping (Figure 4d−f) further reveals that Fe is localized in the outside shell of the vesicle, suggesting that dumbbell nanocrystals located at the outer layer of the assembly structure tend to orient their hydrophilic Fe_3O_4 side toward the outside. For the dumbbell nanocrystals inside the structure, the orientation preference is not obvious, possibly because the collapse during the drying process obscures the orientation. The images suggest that directional interactions still dominate during the assembly, producing vesicle-like structures with Au lobes in contact with each other while the hydrophilic Fe_3O_4 lobe facing outside, providing the stability for these structures in aqueous solutions. The vesicle-like structures are often formed by surfactant or lipid molecules with a certain hydrophilic-lipophilic balance (HLB) value.[39] Simulation on Janus spheres also suggests that in order to form vesicle structures, the hydrophobic side needs to be slightly bigger than the hydrophilic side.[33] There is a narrow range of Janus balance that warrants assembly into vesicles. Indeed, in our dumbbell nanocrystal platform we only observed vesicle structures when using the bulkier polystyrene (rather than the oleylamine) as the hydrophobic coating on the dumbbell nanocrystals with bigger Au lobes (Fe_3O_4/Au $\leq$ 1.16). No vesicle structures were ever observed with dumbbell nanocrystals (Fe_3O_4/Au > 1.16) with smaller hydrophobic Au lobes coated with polystyrene molecules.

The third strategy is to control self-assembly by adjusting the pH of the solution. Unlike those nanoparticles capped by polyethylene glycol for the stabilization in aqueous solutions,[32] our Janus Au−Fe_3O_4 dumbbell nanocrystals take advantage of carboxylic group, which offers a unique way to control the self-assembly. Considering the deprotonation and protonation of carboxylic groups on the Fe_3O_4 lobe, Janus balance of Au−Fe_3O_4 nanoparticles can be further fine-tuned by pH values of the aqueous solution. Switching the Fe_3O_4 lobe from deprotonated state to protonated state will effectively shut down the electrostatic repulsion and induce the assembly of Janus Au−Fe_3O_4 dumbbell nanoparticles. In a typical experiment, Au−Fe_3O_4 dumbbell nanocrystals were modified and initially dispersed in basic solution with pH of 8. The pK_a of 3,4-dihydroxybenzoic acid (~4.2) indicates that carboxylic groups on Fe_3O_4 surfaces are fully deprotonated at pH 8 (Figure S2). The negative charges prevent the Janus particles from assembling. As shown in Figure 5a, Janus Au−Fe_3O_4 nanocrystals were randomly distributed without obvious orientation in the basic solution. When the pH is adjusted to 4, a large amount of carboxylic groups are protonated, which significantly suppresses the surface charges on the Fe_3O_4 lobes. As a result, Janus nanoparticles were no longer stable and started to aggregate. Figure 5b displays the typical aggregation from the solution under pH 4 and clearly indicates the self-assembly was triggered by decreasing the pH value. It is worth pointing out that small clusters (e.g., dimers, trimers, and tetramers) were formed together with the larger aggregates with Au lobes facing each other. Such features suggest that attractions between Au lobes become dominant when the pH

DOI: 10.1021/acs.nanolett.8b04464
Nano Lett. XXXX, XXX, XXX−XXX

decreases. The reduced charge on the Fe_3O_4 lobe allows dumbbell nanocrystals to approach and engage with each other in a shorter distance. Additionally, the assembly process is highly reversible, which is revealed by the UV−vis spectra of the nanoparticle solution oscillating between low and high pH values. As shown in Figure 5c, at pH 8, the solution is in an assembly-OFF state. The UV−vis spectrum exhibits a peak at 529 nm caused by the localized surface plasmon resonance (LSPR) of the Au lobe. At pH 4, the solution is in an assembly-ON state, and the spectrum peak shifts toward 539 nm. Because LSPR is extremely sensitive to the distances between Au surfaces,[40] the red-shift suggests that the gap between Au lobes is narrowed and interparticle plasmonic coupling is improved. This is further corroborated by the TEM images in Figure 5b. The assembly-OFF/ON states were tuned back and forth for three cycles, and the spectra were consistently reproduced for both states as shown in Figure 5d.

In addition, absorbance intensity was kept constant during the three cycles, which suggests the assembly structures are highly reversible. Understandably, the assembled Janus dumbbell nanocrystals are much more responsive to an external magnetic field, which is attributed to the enhanced magnetic response by the Fe_3O_4 domains in the assembly structures (Figure S3).

LSPR effect has been widely studied for homogeneous nanoparticle systems and applied in sensing[41,42] and surface-enhanced Raman spectroscopy.[43,44] The adsorption in the near-infrared region can be used to heat up the surroundings and developed into novel therapeutic methods for treating diseases.[45−47] The Janus Au−Fe_3O_4 dumbbell nanocrystal platform offers a unique approach to modulate the LSPR effect by controlling the interparticle coupling through the Au lobes. In order to further enhance the LSPR effect of the dumbbell nanocrystals, we grow additional Au nanodomains on the Au lobes and achieved the new Au−Au−Fe_3O_4 nanocrystals as shown in Figure 6a. The extrusion of additional Au nanocrystal domains on the Au lobe is realized by reducing Au precursors in the presence of Au−Fe_3O_4 dumbbell nanocrystals. Au nucleation and subsequent growth are more favorable on the Au surface than Fe_3O_4 because of the lattice mismatch. Small Au domains are only observed on the Au lobe, whereas no Au growth is detected on the Fe_3O_4 lobe. Although the growth of the small Au domains is not entirely homogeneous due to the random nucleation on the preformed Au lobe, this unique Au-on-Au lobe morphology nonetheless further enlarges the Au lobe and renders the dumbbell nanoparticles with an even smaller Fe_3O_4/Au ratio that is difficult to achieve with other synthetic methods. Self-assembly of Janus Au−Au−Fe_3O_4 nanocrystals resulted in capsule-like structures with large domains containing interconnected Au lobes as shown in Figure 6b. Similar assembly structures have not been reported with micron-sized Janus particles, although the worm-like micelle structures have been studied with small molecular systems.[48] Obviously the unique morphology of Au−Au−Fe_3O_4 plays an important role in determining the final assembly structures.

When compared with UV−vis spectra of assembly structures formed by other Janus dumbbell nanocrystals (Figure 6c), the LSPR peak of Au−Au−Fe_3O_4 superstructures is much more red-shifted and broader, even reaching into the near-infrared region, indicating greatly enhanced interparticle plasmonic coupling. It is obvious that more Au lobes are contacting each other in the capsules, as shown in Figure 6a. The dark blue

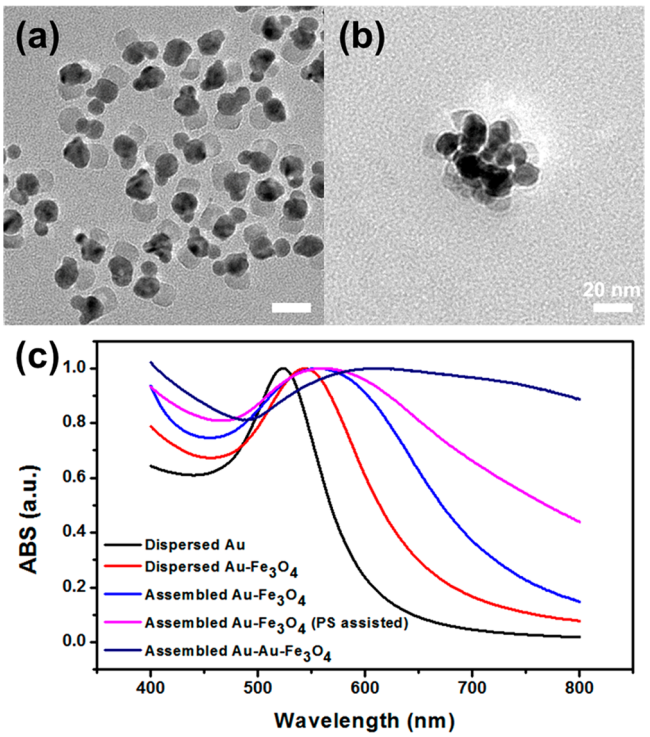

Figure 6. (a) TEM image of Janus Au−Au−Fe_3O_4 nanocrystals obtained by growing Au nanocrystal domains on Au−Fe_3O_4 dumbbell nanocrystals. (b) Self-assembly of Janus Au−Au−Fe_3O_4 nanocrystals shows large domains of Au lobes interconnecting with each other. (c) Comparison of UV−vis spectra of structures assembled from different Janus nanocrystals. The structures assembled with larger hydrophobic moiety lead to stronger LSPR effect.

color of the solution (Figure S4a) also suggests the enhanced interparticle coupling. This is consistent with the trend in Figure 6c that structures assembled with larger hydrophobic moiety lead to stronger LSPR effect (Au−Au−Fe_3O_4 > polystyrene modified Au−Fe_3O_4 > oleylamine modified Au−Fe_3O_4). In addition, assembled Au−Au−Fe_3O_4 nanocrystals is the most responsive under the external magnetic field compared to other Au−Fe_3O_4 dumbbell nanocrystals studied in this paper (Figure S4). The novel Au−Au−Fe_3O_4 nanocrystals offer more flexibility in further extending the dumbbell nanocrystal morphology and controlling the assembly structures. Because of its extraordinarily enhanced surface plasmon performance, the novel Au−Au−Fe_3O_4 nanocrystals may find applications in areas such as sensing and biomedication.

In this work, we have built a Janus dumbbell nanocrystal platform and demonstrated multiple strategies to control the self-assembly of Janus particles at the nanometer length scale. The asymmetric modification of Au−Fe_3O_4 dumbbell nanocrystals enables directional interactions between individual nanoparticles and results in assembly structures balancing Au lobe attraction and Fe_3O_4 lobe repulsion. Furthermore, the self-assembly is effectively controlled by the Fe_3O_4/Au size ratio, size of molecules for surface grafting on the Au lobe, and pH of the solution. A series of structures including small clusters, chains, vesicles and capsules were obtained through assembly of Janus dumbbell nanoparticles with systematically varied Janus balance. In addition, the assembly can be reversibly controlled by adjusting the solution pH. Finally, unique Au−Au−Fe_3O_4 nanocrystals were synthesized and

DOI: 10.1021/acs.nanolett.8b04464
Nano Lett. XXXX, XXX, XXX−XXX

assembled into capsule-like superstructures, giving a stronger and broader LSPR band extending into the near-infrared region. The study here reveals the principles that guide the assembly structures of Janus nanoparticles in terms of Janus balance of individual Janus particles. These assembly structures can enhance the functionality including magnetic and surface plasmonic properties, which may be beneficial to many future applications.

■ ASSOCIATED CONTENT

Supporting Information

The Supporting Information is available free of charge on the ACS Publications website at DOI: 10.1021/acs.nanolett.8b04464.

Experimental details and figures including self-assembly of Janus Au−Fe_3O_4 dumbbell nanocrystals with Fe_3O_4/Au lobe size ratio of 1.16; calculated percentage of deprotonated and protonated carboxylic group under different pH conditions; magnetic response of unassembled and assembled Janus nanocrystals; RAFT polymerization reaction conditions for polystyrene synthesis (PDF)

■ AUTHOR INFORMATION

Corresponding Author

*E-mail: sjiang1@iastate.edu.

ORCID

Michael Forrester: 0000-0003-3063-9975

Tao Ma: 0000-0002-0579-8045

Shan Jiang: 0000-0001-8119-9012

Notes

The authors declare no competing financial interest.

■ ACKNOWLEDGMENTS

S.J. would like to thank Iowa State University for the Start-up Fund and 3M for the Nontenured Faculty Award. L.Z. would like to thank Laboratory Directed Research and Development funds through Ames Laboratory. Some of the TEM-related work was performed using instruments in the Sensitive Instrument Facility in Ames Laboratory. Ames Laboratory is operated for the U.S. Department of Energy by Iowa State University under Contract No. DE-AC02-07CH11358.

■ REFERENCES

(1) Whitesides, G. M.; Grzybowski, B. *Science* **2002**, *295* (5564), 2418−2421.

(2) Boles, M. A.; Engel, M.; Talapin, D. V. *Chem. Rev.* **2016**, *116* (18), 11220−11289.

(3) Vogel, N.; Retsch, M.; Fustin, C. A.; del Campo, A.; Jonas, U. *Chem. Rev.* **2015**, *115* (13), 6265−6311.

(4) Grzybowski, B. A.; Fitzner, K.; Paczesny, J.; Granick, S. *Chem. Soc. Rev.* **2017**, *46* (18), 5647−5678.

(5) Darling, S. B. *Prog. Polym. Sci.* **2007**, *32* (10), 1152−1204.

(6) Degennes, P. G. *Rev. Mod. Phys.* **1992**, *64* (3), 645−648.

(7) Walther, A.; Muller, A. H. E. *Chem. Rev.* **2013**, *113* (7), 5194−5261.

(8) Hu, J.; Zhou, S.; Sun, Y.; Fang, X.; Wu, L. *Chem. Soc. Rev.* **2012**, *41* (11), 4356−4378.

(9) Zhang, J.; Grzybowski, B. A.; Granick, S. *Langmuir* **2017**, *33* (28), 6964−6977.

(10) Kang, C. J.; Honciuc, A. *ACS Nano* **2018**, *12* (4), 3741−3750.

(11) Hong, L.; Cacciuto, A.; Luijten, E.; Granick, S. *Nano Lett.* **2006**, *6* (11), 2510−2514.

(12) Chen, Q.; Whitmer, J. K.; Jiang, S.; Bae, S. C.; Luijten, E.; Granick, S. *Science* **2011**, *331* (6014), 199−202.

(13) Chen, Q.; Bae, S. C.; Granick, S. *Nature* **2011**, *469* (7330), 381−384.

(14) Palacci, J.; Sacanna, S.; Steinberg, A. P.; Pine, D. J.; Chaikin, P. M. *Science* **2013**, *339* (6122), 936−940.

(15) Buttinoni, I.; Bialke, J.; Kummel, F.; Lowen, H.; Bechinger, C.; Speck, T. *Phys. Rev. Lett.* **2013**, *110* (23), 238301.

(16) Berger, S.; Synytska, A.; Ionov, L.; Eichhorn, K. J.; Stamm, M. *Macromolecules* **2008**, *41* (24), 9669−9676.

(17) Gangwal, S.; Cayre, O. J.; Velev, O. D. *Langmuir* **2008**, *24* (23), 13312−13320.

(18) Ma, F. D.; Wang, S. J.; Wu, D. T.; Wu, N. *Proc. Natl. Acad. Sci. U. S. A.* **2015**, *112* (20), 6307−6312.

(19) Zerrouki, D.; Baudry, J.; Pine, D.; Chaikin, P.; Bibette, J. *Nature* **2008**, *455* (7211), 380−382.

(20) Yan, J.; Bloom, M.; Bae, S. C.; Luijten, E.; Granick, S. *Nature* **2012**, *491* (7425), 578−81.

(21) Yu, H.; Chen, M.; Rice, P. M.; Wang, S. X.; White, R. L.; Sun, S. H. *Nano Lett.* **2005**, *5* (2), 379−382.

(22) Xu, C. J.; Wang, B. D.; Sun, S. H. *J. Am. Chem. Soc.* **2009**, *131* (12), 4216.

(23) Liu, S.; Guo, S. J.; Sun, S.; You, X. Z. *Nanoscale* **2015**, *7* (11), 4890−4893.

(24) Wu, B. H.; Tang, S. H.; Chen, M.; Zheng, N. F. *Chem. Commun.* **2014**, *50* (2), 174−176.

(25) Jiang, G. M.; Huang, Y. X.; Zhang, S.; Zhu, H. Y.; Wu, Z. B.; Sun, S. H. *Nanoscale* **2016**, *8* (41), 17947−17952.

(26) Lattuada, M.; Hatton, T. A. *J. Am. Chem. Soc.* **2007**, *129* (42), 12878−12889.

(27) Sardar, R.; Heap, T. B.; Shumaker-Parry, J. S. *J. Am. Chem. Soc.* **2007**, *129* (17), 5356−7.

(28) Ikegami, S.; Yamaguchi, K.; Tanaka, T.; Takeyasu, N.; Kaneta, T. *Jpn. J. Appl. Phys.* **2018**, *57* (12), 120311.

(29) Wang, C.; Xu, C. J.; Zeng, H.; Sun, S. H. *Adv. Mater.* **2009**, *21* (30), 3045−3052.

(30) Hu, H. C.; Ji, F.; Xu, Y.; Yu, J. Q.; Liu, Q. P.; Chen, L.; Chen, Q.; Wen, P.; Lifshitz, Y.; Wang, Y.; Zhang, Q.; Lee, S. T. *ACS Nano* **2016**, *10* (8), 7323−7330.

(31) Jishkariani, D.; Wu, Y.; Wang, D.; Liu, Y.; van Blaaderen, A.; Murray, C. B. *ACS Nano* **2017**, *11* (8), 7958−7966.

(32) Song, J. B.; Wu, B. H.; Zhou, Z. J.; Zhu, G. Z.; Liu, Y. J.; Yang, Z.; Lin, L. S.; Yu, G. C.; Zhang, F. W.; Zhang, G. F.; Duan, H. W.; Stucky, G. D.; Chen, X. Y. *Angew. Chem., Int. Ed.* **2017**, *56* (28), 8110−8114.

(33) Miller, W. L.; Cacciuto, A. *Phys. Rev. E* **2009**, *80* (2), 021404.

(34) Huang, H. Y.; Chen, W. F.; Kuo, P. L. *J. Phys. Chem. B* **2005**, *109* (51), 24288−24294.

(35) Ohno, K.; Koh, K.; Tsujii, Y.; Fukuda, T. *Angew. Chem.* **2003**, *115* (24), 2857−2860.

(36) Ye, X. C.; Zhu, C. H.; Ercius, P.; Raja, S. N.; He, B.; Jones, M. R.; Hauwiller, M. R.; Liu, Y.; Xu, T.; Alivisatos, A. P. *Nat. Commun.* **2015**, *6*, 10052.

(37) Liu, K.; Nie, Z. H.; Zhao, N. N.; Li, W.; Rubinstein, M.; Kumacheva, E. *Science* **2010**, *329* (5988), 197−200.

(38) Choueiri, R. M.; Galati, E.; Therien-Aubin, H.; Klinkova, A.; Larin, E. M.; Querejeta-Fernandez, A.; Han, L. L.; Xin, H. L.; Gang, O.; Zhulina, E. B.; Rubinstein, M.; Kumacheva, E. *Nature* **2016**, *538* (7623), 79−83.

(39) Uchegbu, I. F.; Florence, A. T. *Adv. Colloid Interface Sci.* **1995**, *58* (1), 1−55.

(40) Klinkova, A.; Choueiri, R. M.; Kumacheva, E. *Chem. Soc. Rev.* **2014**, *43* (11), 3976−3991.

(41) Saha, K.; Agasti, S. S.; Kim, C.; Li, X. N.; Rotello, V. M. *Chem. Rev.* **2012**, *112* (5), 2739−2779.

(42) Lee, K. S.; El-Sayed, M. A. *J. Phys. Chem. B* **2006**, *110* (39), 19220−19225.

DOI: 10.1021/acs.nanolett.8b04464
Nano Lett. XXXX, XXX, XXX−XXX

(43) Talley, C. E.; Jackson, J. B.; Oubre, C.; Grady, N. K.; Hollars, C. W.; Lane, S. M.; Huser, T. R.; Nordlander, P.; Halas, N. J. *Nano Lett.* **2005**, *5* (8), 1569−1574.
(44) Li, J. F.; Huang, Y. F.; Ding, Y.; Yang, Z. L.; Li, S. B.; Zhou, X. S.; Fan, F. R.; Zhang, W.; Zhou, Z. Y.; Wu, D. Y.; Ren, B.; Wang, Z. L.; Tian, Z. Q. *Nature* **2010**, *464* (7287), 392−395.
(45) Dreaden, E. C.; Alkilany, A. M.; Huang, X. H.; Murphy, C. J.; El-Sayed, M. A. *Chem. Soc. Rev.* **2012**, *41* (7), 2740−2779.
(46) Jain, P. K.; El-Sayed, I. H.; El-Sayed, M. A. *Nano Today* **2007**, *2* (1), 18−29.
(47) Boisselier, E.; Astruc, D. *Chem. Soc. Rev.* **2009**, *38* (6), 1759−1782.
(48) Cates, M. E.; Candau, S. J. *J. Phys.: Condens. Matter* **1990**, *2* (33), 6869.

DOI: 10.1021/acs.nanolett.8b04464
Nano Lett. XXXX, XXX, XXX−XXX